Automatic Parameters Optimization for Deep Brain Stimulation Trajectory Planning

Caroline Essert[1], Maud Marchal[2], Sara Fernandez-Vidal[3], Tiziano D'Albis[4], Eric Bardinet[3], Claire Haegelen[5], Marie-Laure Welter[6], Jérôme Yelnik[3], and Pierre Jannin[4]

[1] LSIIT / Université de Strasbourg, France
[2] Inria Rennes / INSA, France
[3] CENIR - ICM Paris, France
[4] LTSI, Inserm / Université Rennes 1, France
[5] Hôpital Pontchaillou, Department of neurosurgery, Rennes, France
[6] Hôpital Pitié-Salpêtrière, Department of neurology, Paris, France
`essert@unistra.fr`

Abstract. In this paper, we propose an approach aiming at optimizing the parameters of automatic trajectory computation methods in Deep Brain Stimulation. Such methods are usually based on the search for a trajectory that optimizes surgical constraints or risk maps. Such constraints are combined together with a weighting related to their respective importance. Usually, the weights are fixed empirically, in cooperation with the surgeons. The proposed approach aims at refining the weighting factors using a learning process on retrospective cases, in order to fit at best the weights that are closer to the surgeons expertise. We present how this approach has been applied with success on a preoperative electrode trajectory optimization tool. This preliminary work, based on one patient case, shows that it is possible to retrieve the weights corresponding to a given performed trajectory.

1 Introduction

Deep Brain Stimulation (DBS) is one surgical answer to Parkinson's disease or essential tremors for patients with severe symptoms who do not respond well to medication. The intervention consists in implanting one (or several) electrode(s) into deep locations of the brain for electric stimulation causing an inhibition of the motor disorders. This treatment is very efficient but the planning still challenging. The planning phase mainly relies on the study of images (such as MRI and CT), acquired before the intervention. Its objectives are to accurately locate the anatomical target, which is often not easy to find on usual images, and to find a secure path to the selected target for an electrode to be inserted. This can be a tedious task, for which many neurosurgeons expressed a need for a computer-aided assistance. Many authors also underlined the importance of an accurate planning to avoid risks of side effects [18] or hemorrhage [3].

Recently, several authors reported methods for automatic computation of linear trajectories for DBS electrodes [6, 4, 5, 13, 14]. All approaches are based on constraints to be optimized or risks to be minimized. The constraints or risks are usually defined based on rules expressed by surgeons during interviews and translated into numerical

data based on patient specific multimodal medical images. Then different strategies are defined for computing the optimal trajectory(ies) from such numerical constraints. The constraints are various and expressed different parameters used by the surgeon for selecting the trajectory. For the automatic computation, the methods required the combination of the constraints into a single cost function. The surgical rules do not have the same importance, implying the choice of different values for weighting the constraints within the search for an optimum.

So far, the weights have been chosen empirically by the developers of the methods or at best *a priori* in cooperation with the neurosurgeons. In order to follow a more objective approach, Liu et al. proposed in [9] an approach for adapting the weighting factors to single surgeon. However, the computation of the optimal values for the weights was done manually by subjective analysis of the computed trajectories. In this paper, we present the theoretical aspects of a generic and objective approach to retrieve automatically the weighting factors corresponding to a chosen electrode trajectory, based on a Bayesian strategy. The *a posteriori* method is based on the post-operative analysis of a patient case. We show the feasibility of the approach be applying it to a method of DBS electrode trajectory computation we previously published [6] and for one patient's case. Then we discuss how this method will be used in further works with larger sets of patients to learn the most accurate weights for a neurosurgeon by learning from his/her past cases, and to analyze the difference that could occur between surgeons, between medical centers, or between patients.

2   Materials and Methods

2.1   Automatic Determination of Weights from Post-operative Images

Bayesian Approach The solving process of our trajectory planning method solves a linear combination of four cost functions f_1 to f_4 (for details about the used cost functions, please refer to [6]). This linear combination can be seen as a *main cost function f* to minimize, with weighting factors w_1 to w_4 assigned to each individual cost function:

$$f = \frac{w_1.f_1 + w_2.f_2 + w_3.f_3 + w_4.f_4}{w_1 + w_2 + w_3 + w_4}$$

When launched with fixed values for the weights, we obtain a set of candidate trajectories that satisfy the constraints. The trajectory T_{opt} providing the lowest result $r_{opt} = f(w_1, w_2, w_3, w_4, T_{opt})$ is indicated as the optimal trajectory.

The main hypothesis of methods that automatically compute optimal trajectories is that, for every trajectory chosen by a surgeon, it exists a set of weights that allows the automatic estimation of this trajectory. If we want to find these weights, we need to try all possible combinations of weights, and launch for each one an optimization process. For at least one of the experimented combinations, the optimal solution will fit the trajectory manually chosen by the surgeon. Experimenting all possible combinations would be very time-consuming. Indeed, if we consider that we currently have 4 weights to combine, and if we want to have a precision of 0.01 per weight, the optimization process taking about 0.25 second per combination, it means that it will take

about $100^4 * 0.25$ seconds to compute, which represents nearly $7,000$ hours. To reduce the computation time, we could have decreased the precision of the weights. We chose instead to use a Bayesian approach allowing an efficient browsing of the entire space of combinations while keeping a very good precision and a reasonable computation time.

The algorithm consists in first defining a maximum number of combinations i_{max} that will be tested. We set i_{max} at $10,000$, leading to a computation time of approximately 40 minutes. Then, we start looping over weights combinations. At each step i, we assign new values w_{i1} to w_{i4} for the four weights, randomly chosen between 0 and 1 with a precision of 3.10^{-5}. We launch the optimization process with the fixed weights, and the trajectory converges to trajectory T_{iopt} having the smallest result $r_{iopt} = f(w_{i1}, w_{i2}, w_{i3}, w_{i4}, T_{iopt})$ for the main cost function. We compute the angle α_i between the trajectory actually performed by the surgeon T_{real} and T_{iopt}. Then we compare α_i with the smallest angle α_{min} found so far: if α_i is smaller, then we memorize this candidate trajectory as the nearest to the objective, i.e. we memorize weights w_{i1} to w_{i4} and the associated angle α_i becomes the new α_{min}. The loop stops when i reaches i_{max}. At the end of the loop, if α_{min} is under 0.1 degree, we can reasonably consider that we have found a candidate trajectory close enough to the trajectory actually chosen by the surgeon, and therefore the associated combination of weights.

Search among the x most Optimal Trajectories In our software, all candidate trajectories are represented as a map of colored entry points on the skin (Fig.1). The color of each entry point depends on the result of the cost function for the corresponding trajectory. When visualizing the color map, we can observe colored valleys. They are centered around the x best trajectories T_x with a result of the main cost function very close to the optimal trajectory, *i.e.* for which the result r_x is such that $r_x - r_{opt} < \varepsilon$. It can happen that the difference between the x best trajectories and the optimal trajectories is insignificant. Therefore, we can suppose that the trajectory actually chosen by the neurosurgeon T_{real} might as well be one of those.

To take this observation into account, we extended our search to the x most optimal trajectories. The valleys are computed as the connected components (CC) within the search area inside which all entry points lead to a result r for f such that $r - r_{opt} < \varepsilon$ (Fig.2). For a particular set of weights, according to the choice of ε the number of CC might not be the same: a higher value of ε increases the number of trajectories considered as one of the "best", as well as the size of the valley surrounding it. Reciprocally, for a particular ε, a different choice of weights combination can modify the number of CC: valleys do not have the same shape, size or location, and some connected components can appear, disappear, merge or split. As a consequence, for each step i of the main loop the value of ε needs to be adjusted so that the number x of considered best trajectories is always equal.

Optimizing x trajectories instead of one at each step increases the computation time approximately by x. Therefore, to stay under the hour of computation, we tried different combinations of x and i_{max}, still keeping the same precision for the weights. Details of the experimented values and the obtained results are given in Section 3.
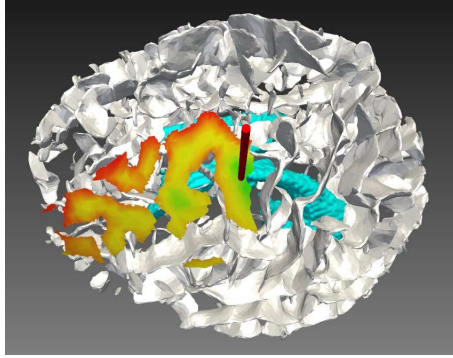
Fig. 1. Snapshot showing the map of colored entry points on the skin resulting from the solving process. In white, the cortical sulci. The ventricles are in blue. The STN is hidden by a sulcus. The electrode computed as optimal is in red. On the color map, the best entry points are shown in green and the worst are in red, with intermediate colors for entry points with medium results. We can observe 2 large and 1 very small green valleys.

2.2 Data

In this section, we explain the set of data and the image processing algorithms and pipelines we used in order to test our method. For now, it has been tested on one patient, and the results are shown in Section 3. However, the algorithms and pipelines are reproducible on any patient image, and will be used in future statistical studies to obtain sets of optimal weights on numerous patients.

For the solving process, we first need 3D meshes of the ventricles and the vessels, which are the main critical structures to avoid. If the vessels cannot be segmented with a sufficient quality, we use instead the 3D mesh of the cortical sulci, as surgeons often do in the current clinical routine, since most of the vessels are located inside the sulci. Additionally, we need the 3D meshes of the targets, in our case the left and right SubThalamic Nucleus (STN). Finally, we need an initial search area for the entry point of the electrode, *i.e.* a 3D mesh of a selected portion of the scalp. All these anatomical structures can be processed from the pre-operative 3T T1-weighted MRI (1 mm x 1 mm x 1 mm, Philips Medical Systems), acquired just before the intervention.

The segmentation of scalp and cortical sulci and the generation of the associated triangle meshes were done automatically through the BrainVISA [12] anatomical segmentation pipeline [11]. Volumetric segmentation of the ventricular system was performed through the Freesurfer image analysis suite. Specifically, we used the FreeSurfer pipeline dedicated to the subcortical segmentation of deep structures [7], from which the volumetric masks of the two lateral ventricles and the third and fourth ventricles were extracted. The corresponding surface triangle meshes were generated using the BrainVISA AIMS software library [12].

From the triangle mesh of the scalp, the initial area on the skin is defined interactively using the Paraview viewer from Kitware [8] by selecting a portion of the mesh located on the concerned side of the head. Ideally, this portion has to be wide enough

(a) 3 connected components   (b) 5 connected components
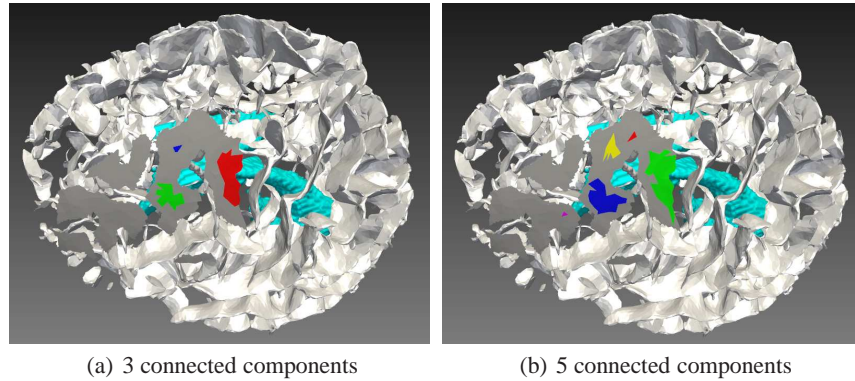
Fig. 2. Snapshots showing the x connected components on the skin mesh, representing the valleys around the x best trajectories. Corresponding colored valleys can be seen on Fig.1.

not to be too restrictive. However, the insertion point should remain anterior to the precentral sulcus, posterior to the hair area, and not too close to the ear area. Therefore, we use those limits to define the initial area for each side of the bilateral implantation.

Three-dimensional meshes of the targets (STN) were obtained by registering the YeB atlas on the patient T1-weighted MR images. The YeB atlas is a three-dimensional and histological atlas of the basal ganglia [17] that consists of a set of 3D meshes representing the basal ganglia. It has been used for pre-operative definition of targets [1], peroperative localization of electrophysiological recordings and post-operative anatomical identification of stimulation electrode contacts [15]. The YeB atlas was built from a post-mortem specimen, and also includes post-mortem MR acquisitions of the head. This atlas can be adapted to the brain of a specific patient, by a deformation strategy based on iconic registrations between the post-mortem and the patient T1-weighted MR images [2]. The resulting transformation is then applied to the basal ganglia 3D meshes in the post-mortem atlas space, providing an individual cartography of the patient's basal ganglia.

Finally, we need the location of the trajectory actually chosen by the surgeon T_{real}. The electrode can be segmented from the post-operative CT scan (0.44 mm x 0.44 mm x 0.6 mm for post-operative acquisitions, GE Healthcare VCT 64), acquired few days after the intervention. A rigid registration of the post-operative CT on the pre-operative MRI is performed using Newuoa optimization [16] with Mutual Information as cost function. Then, we interactively segment the electrode on the CT and we extract a 3D mesh from the segmented shape, thanks to MITK [10] functionalities. From this shape, we extract the main axis of the electrode by using a Principal Component Analysis (PCA) (Fig.3(b)).

A snapshot showing all the anatomical structures we used after they are processed and reconstructed as 3D meshes is shown on Fig.3(a).

(a) Full 3D scene   (b) T_{real}
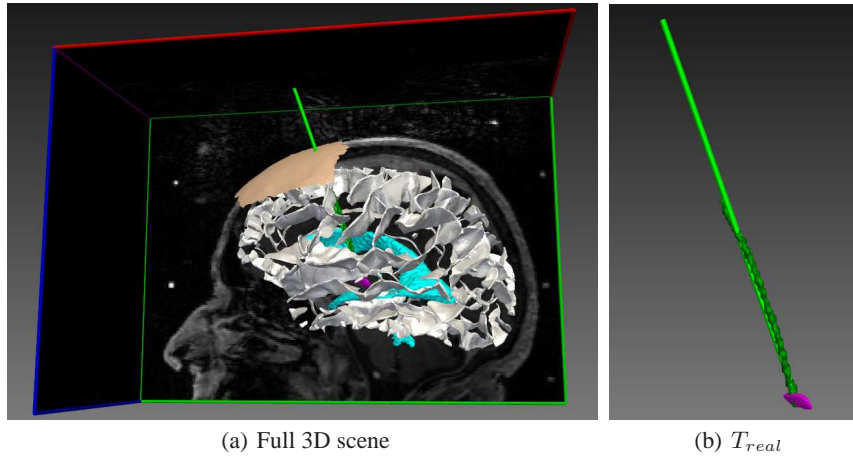
Fig. 3. Snapshot showing the data. In the background, the pre-operative MRI. In white, the cortical sulci. The ventricles are in blue and the STN is in pink. The electrode segmented from the registered post-operative CT is in dark green, and the extracted main axis is in light green. On the top of the head, the initial zone is in orange.

3 Results

We experimented our approach on one patient with a bilateral STN stimulation. We applied the image processing pipelines described in Paragraph 2.2 to obtain the triangle meshes, and delineated two patches on the skin on both sides of the head to define initial areas of interest. We present here the results for the left hemisphere.

For both sides, we applied our method for finding weights with the following values of x: 1, 3 and 5. For each one, we chose a value of i_{max} allowing us to keep the computation time under one hour: $i_{max} = 10,000$ for $x = 1$, $i_{max} = 5,000$ for $x = 3$, and $i_{max} = 3,000$ for $x = 5$. Table 1 summarizes the results we obtained for those combinations, for the 10 trajectories closest to T_{real}. Snapshots illustrating the results are shown on Fig.4. Computation times were respectively 36.51 min. for $x = 1$, 51.77 min. for $x = 3$, and 31 min. for $x = 5$ for the left hemisphere. For the latest, the computation time was lower because some configurations could not provide 5 connected components and were quickly rejected.

On Table 1, we can see that with $x = 1$ (*i.e.* if we consider only the most optimal candidate trajectory) we can not find any combination of weights leading to an approximation of T_{real}. When extending the search to the 3 best connected components ($x = 3$), we obtain combinations of weights leading to trajectories very close to T_{real}. The average difference of 0.068 degrees can be considered as quite insignificant compared to the errors due to the approximation of the segmented electrode. Extending the search to the 5 best connected components ($x = 5$) does not seem in this case to be significant, as it does not provide trajectories closer to T_{real}.

We can notice that with $x = 3$ or $x = 5$ all the trajectories belong to the same connected component (even for trajectory #1 of $x = 5$, where the connected component

Table 1. Results of the automatic computation of the combinations of weights leading to the "best" trajectories closest to T_{real}. The first column indicates the conditions of the experiment, *i.e.* the value of x. Then, for each condition, we show the weights w_{j1} to w_{j4} of the 4 constraints for the $j = 0, \ldots, 10$ best trajectories T_j. For each T_j, we also show the number of the connected component (CC) in which T_j is located, the angle α_j between T_j and T_{real}, and the result r_j. For comparison, we also show r_{opt} and and r_{real}, which are respectively the results of f for the optimal trajectory T_{opt} and for the surgeon's trajectory T_{real} computed with weights fixed with the previously used *a priori* method.

Conditions	best traj. #	w_{j1}	w_{j2}	w_{j3}	w_{j4}	CC #	α_j	r_j	r_{opt}	r_{real}
	1	0.681	0.076	0.925	0.877	1	6.677	0.533		
	2	0.439	0.849	0.553	0.711	1	6.708	0.618		
	3	0.596	0.958	0.710	0.675	1	6.731	0.591		
	4	0.216	0.475	0.256	0.347	1	6.742	0.624		
$x = 1$	5	0.616	0.304	0.714	0.715	1	6.747	0.547		
	6	0.507	0.414	0.983	0.964	1	6.749	0.588		
	7	0.277	0.479	0.441	0.577	1	6.753	0.622		
	8	0.262	0.438	0.532	0.479	1	6.754	0.605		
	9	0.397	0.982	0.863	0.920	1	6.756	0.630		
	10	0.748	0.489	0.976	0.873	1	6.775	0.553		
	1	0.102	0.649	0.502	0.583	3	0.040	0.712		
	2	0.267	0.795	0.956	0.727	3	0.048	0.667		
	3	0.674	0.583	0.882	0.345	3	0.056	0.541		
	4	0.052	0.155	0.593	0.465	3	0.063	0.696		
$x = 3$	5	0.151	0.727	0.504	0.025	3	0.069	0.627	0.595	0.676
	6	0.690	0.679	0.956	0.411	3	0.074	0.555		
	7	0.156	0.207	0.910	0.118	3	0.074	0.584		
	8	0.267	0.281	0.977	0.364	3	0.084	0.602		
	9	0.088	0.602	0.575	0.299	3	0.084	0.680		
	10	0.425	0.045	0.927	0.808	3	0.084	0.609		
	1	0.246	0.701	0.835	0.455	4	0.040	0.647		
	2	0.614	0.317	0.877	0.323	3	0.063	0.523		
	3	0.262	0.331	0.743	0.668	3	0.063	0.652		
	4	0.236	0.482	0.917	0.621	3	0.074	0.654		
$x = 5$	5	0.163	0.743	0.659	0.447	3	0.108	0.675		
	6	0.132	0.389	0.557	0.561	3	0.108	0.689		
	7	0.646	0.533	0.777	0.311	3	0.112	0.534		
	8	0.250	0.670	0.712	0.598	3	0.115	0.663		
	9	0.159	0.276	0.977	0.788	3	0.125	0.679		
	10	0.221	0.581	0.885	0.971	3	0.125	0.691		

is in fact the same but it wasn't numbered the same way). The connected components are numbered according to the ordering of the "best trajectories" around which they are formed, i.e. connected component #1 is around the optimal trajectory, connected component #2 is around the second most optimal trajectory, etc.

(a) $x = 1, i_{max} = 10000$ (b) $x = 3, i_{max} = 5000$ (c) $x = 5, i_{max} = 3000$
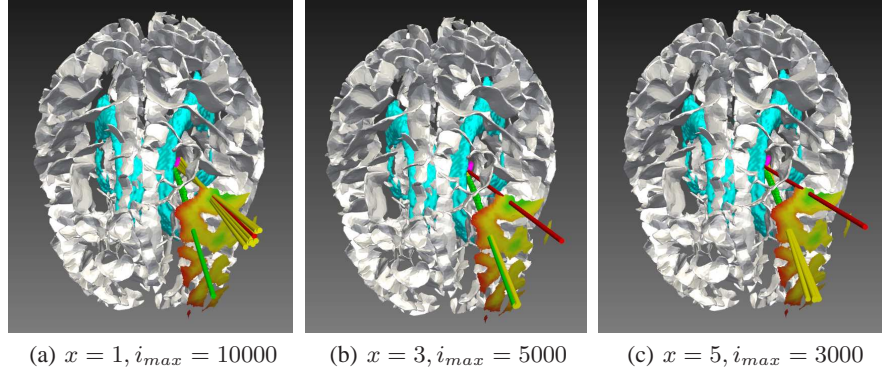
Fig. 4. Snapshots showing the 10 trajectories T_j (in yellow) closest to T_{real} (in green), for different values of x. The combinations of weights leading to these trajectories are detailed in Table 1. The optimal trajectory T_{opt} computed with our default weights is in red.

4 Discussion

One advantage of our approach is that could be easily applied with any trajectory planning method involving a linear combination of cost functions. Moreover, we kept the computation times less than one hour, so that this method could be used on a larger study with many patients cases to process.

Our experiments with 3 different numbers of investigated CC highlights that the surgeon might not always have chosen manually the solution that is numerically computed as the best one. This strengthens our idea that not only one, but several optimal solutions, located in different CC of interest, need to be proposed to the surgeon in a computed-aided help for trajectory planning. Moreover, for the computation of weights, we also need to consider several CCs in case the surgeon didn't choose the one containing the most optimal. We noticed in this first experiment that the surgeon had chosen the third best CC. If we set the weights respectively to $w_{i1} = 0.246$, $w_{i2} = 0.701$, $w_{i3} = 0.835$, and $w_{i4} = 0.455$, which lead to one of the trajectories closest to T_{real}, we obtain respectively a result $r_{CC1} = 0.592$ for the most optimal trajectory (CC #1), $r_{CC2} = 0.625$ for CC #2, and $r_{CC3} = 0.664$ for CC #3 *i.e.* the one including T_{real}. However, the results r of the three best propositions stay within an ε of 0.072.

We can also notice that extending the search to more connected components shows no particular interest. In further works, we could restrict our search directly to the connected component including or being the closest to T_{real}.

On Table 1, when comparing r_j with r_{opt} and r_{real}, we observe that in some cases r_j is smaller than r_{opt}. However, we need to keep in mind that the weights used to compute the different r_j and r_{opt} are not the same: r_{opt} was computed with weights that were fixed with the previously used *a priori* method (basically $w_1 = 0.1$, $w_2 = 0.3$, $w_3 = 0.3$, $w_4 = 0.3$). This observation indicates that those weights we used were probably not chosen optimally. This comforts us in thinking that the weights should not be fixed *a priori*, but should take into account the expertise of the surgeon by learning from his/her past cases, which was the main motivation of this study.

There is no bijection between combinations of weights and location of optimal trajectories. Several combinations of weights can lead to the same trajectory, as well as no combination of weights can lead to the trajectory chosen by the surgeon.

The first situation can happen very often. It is not really annoying if we only want to find at least one combination of weights. It can become an issue if we want to perform a statistical analysis to find recurrent combinations of weights and correlate them with a surgeon, a medical center or a kind of clinical data. In that case some solutions could be to memorize not only the best set of weights but several sets. Our study performed on one patient case already shows that the 10 best combinations leading to trajectories closest to T_{real} are composed of very different weights for each w_i. This underlines the importance to investigate in the future the most recurrent or significant combinations.

The second situation can happen if the surgeon has chosen, maybe exceptionally, a trajectory that does not match the usual surgical rules. For instance, if a patient has severe symptoms but the only way to treat this patient is to take more risks than usual because of the spatial configuration of the brain, the surgeon might sometimes consider taking this risk based on his/her experience, and choose a trajectory that would not be considered by the software as possible. In that case, it will not be possible to find any combination of weights fitting the chosen trajectory.

5 Conclusion

In this paper we presented a new method to automatically estimate the weights of a linear combination of constraints defining the optimal placement of an electrode for DBS. The retrospective approach provides several possible combinations of weights leading to the same electrode trajectory than the one that was chosen in clinical routine by the surgeon. Our approach uses a Bayesian method that performs an extensive search over the parameters space, while avoiding a very time-consuming and less precise exhaustive search. The search is extended to several connected components of the solution space, to be sure to include the objective trajectory.

The approach we presented here could be used with any numerical problem involving a linear combination of functions with weights assigned to each one. We showed in our experiments with one particular trajectory planning process using a linear combination of functions that we could find several candidate combinations of weights. When performed on a large set of patient images, this method could be used for a statistical study to extract recurrent combinations.

Acknowledgments

References

1. Bardinet, E., Belaid, H., Grabli, D., Welter, M.L., Vidal, S.F., Galanaud, D., Derrey, S., Dormont, D., Cornu, P., Yelnik, J., Karachi, C.: Thalamic stimulation for tremor: Can target determination be improved? Movement Disorders 26(2), 307–312 (2011)

2. Bardinet, E., Bhattacharjee, M., Dormont, D., Pidoux, B., Malandain, G., Schüpbach, M., Ayache, N., Cornu, P., Agid, Y., Yelnik, J.: A three-dimensional histological atlas of the human basal ganglia. II. atlas deformation strategy and evaluation in deep brain stimulation for parkinson disease. Journal of Neurosurgery 110(2), 208–219 (2009)

3. Benabid, A., Chabardes, S., Mitrofanis, J., Pollak, P.: DBS of the subthalamic nucleus for the treatment of parkinson's disease. The Lancet Neurology 8(1), 67–81 (2009)

4. Bériault, S., Subaie, F., Mok, K., Sadikot, A., Pike, G.: Automatic trajectory planning of DBS neurosurgery from multi-modal MRI datasets. In: Fichtinger, G., Martel, A., Peters, T. (eds.) proceedings of MICCAI'11, Springer LNCS, vol. 6891, pp. 259–266 (2011)

5. D'Haese, P.F., Pallavaram, S., Li, R., Remple, M.S., Kao, C., Neimat, J.S., Konrad, P.E., Dawant, B.M.: Cranialvault and its crave tools: A clinical computer assistance system for deep brain stimulation (DBS) therapy. Medical Image Analysis 16(3), 744 – 753 (2012)

6. Essert, C., Haegelen, C., Lalys, F., Abadie, A., Jannin, P.: Automatic computation of electrodes trajectories for deep brain stimulation: A hybrid symbolic and numerical approach. Int. J. Comput. Assist. Radiol. Surg. 7(4), 517–532 (2012)

7. Fischl, B., Salat, D.H., van der Kouwe, A.J., Makris, N., Ségonne, F., Quinn, B.T., Dale, A.M.: Sequence-independent segmentation of magnetic resonance images. NeuroImage 23, Supplement 1, S69 – S84 (2004)

8. Henderson, A.: ParaView Guide, A Parallel Visualization Application. Kitware Inc. (2007)

9. Liu, Y., Dawant, B.M., Pallavaram, S., Neimat, J.S., Konrad, P.E., D'Haese, P.F., Datteri, R.D., Landman, B.A., Noble, J.H.: A surgeon specific automatic path planning algorithm for deep brain stimulation. In: proceedings of SPIE Medical Imaging 2012: Image-Guided Procedures, Robotic Interventions, and Modeling. p. 83161D (2012)

10. Maleike, D., Nolden, M., Meinzer, H., Wolf, I.: Interactive segmentation framework of the medical imaging interaction toolkit. Computer methods and programs in biomedicine 96(1), 72–83 (2009), http://www.mitk.org

11. Mangin, J.F., Rivière, D., Cachia, A., Duchesnay, E., Cointepas, Y., Papadopoulos-Orfanos, D., Scifo, P., Ochiai, T., Brunelle, F., Régis, J.: A framework to study the cortical folding patterns. Neuroimage 23, S129–S138 (2004)

12. Rivière, D., Geffroy, D., Denghien, I., Souedet, N., Cointepas, Y.: BrainVISA: an extensible software environment for sharing multimodal neuroimaging data and processing tools. In: Neuroimage. vol. 47, pp. 163–163 (2009)

13. Shamir, R., Tamir, I., Dabool, E., Joskowicz, L., Shoshan, Y.: A method for planning safe trajectories in image-guided keyhole neurosurgery. In: proceedings of MICCAI'10. vol. 6363, pp. 457–464. Springer LNCS (2010)

14. Tirelli, P., d.M.E.B.N.F.G.: An intelligent atlas-based planning system for keyhole neurosurgery. In: Computer Assisted Radiology and Surgery supplemental. pp. S85–S91 (2009)

15. Welter, M.L., Burbaud, P., Fernandez-Vidal, S., Bardinet, E., Coste, J., Piallat, B., Borg, M., Besnard, S., Sauleau, P., Devaux, B., Pidoux, B., Chaynes, P., Tézenas du Montcel, S., Bastian, A., Langbour, N., Teillant, A., Haynes, W., Yelnik, J., Karachi, C., Mallet, L.: Basal ganglia dysfunction in OCD: subthalamic neuronal activity correlates with symptoms severity and predicts high-frequency stimulation efficacy. Translational Psychiatry 1(e5) (2011)

16. Wiest-Daesslé, N., Yger, P., Prima, S., Barillot, C.: Evaluation of a new optimisation algorithm for rigid registration of MRI data. In: SPIE Medical Imaging. p. 651206 (2007)

17. Yelnik, J., Bardinet, E., Dormont, D., Malandain, G., Ourselin, S., Tandé, D., Karachi, C., Ayache, N., Cornu, P., Agid, Y.: A three-dimensional, histological and deformable atlas of the human basal ganglia. I. atlas construction based on immunohistochemical and mri data. NeuroImage 34(2), 618 – 638 (2007)

18. York, M.K., Wilde, E.A., Simpson, R., Jankovic, J.: Relationship between neuropsychological outcome and DBS surgical trajectory and electrode location. Journal of the Neurological Sciences 287(1-2), 159 – 171 (2009)